

PROCEEDINGS OF SPIE

SPIDigitalLibrary.org/conference-proceedings-of-spie

Modeling disease agents transmission dynamics in dementia on heterogeneous spatially embedded networks

Tahmassebi, Amirhessam, Karbaschi, Gelareh, Meyer-Baese, Uwe, Meyer-Baese, Anke

Amirhessam Tahmassebi, Gelareh Karbaschi, Uwe Meyer-Baese, Anke Meyer-Baese, "Modeling disease agents transmission dynamics in dementia on heterogeneous spatially embedded networks," Proc. SPIE 11735, Pattern Recognition and Tracking XXXII, 117350N (12 April 2021); doi: 10.1117/12.2588294

SPIE.

Event: SPIE Defense + Commercial Sensing, 2021, Online Only

Modeling Disease Agents Transmission Dynamics in Dementia on Heterogeneous Spatially Embedded Networks

Amirhessam Tahmassebi^a, Gelareh Karbaschi^b, Uwe Meyer-Baese^c, and Anke Meyer-Baese^a

^aDepartment of Scientific Computing, Florida State University, Tallahassee, FL, USA

^bDepartment of Computer Information Technology & Graphics, Purdue University Northwest
Hammond, IN, USA

^cDepartment of Electrical and Computer Engineering, Florida A&M University and Florida
State University, Tallahassee, FL, USA

ABSTRACT

Current models for determining dementia progression are network diffusion models derived from the heat equation without diffusion sources, and they do not model the disease agents (misfolded β -amyloid and τ -protein) transmission dynamics. In this paper, we derive from a SIRI (Susceptible-Infected-Recovered-Infected) epidemic model a simplified model under the information-centric paradigm over a network of heterogeneous agents and including the long-range dispersal of disease agents. The long-range disease agent dispersal is implemented by including the Mellin and Laplace transforms in the adjacency matrix of the graph network. We analyze the influence of different transforms on the epidemic threshold which shows when a disease dies off. Further we analyze the dynamical properties of this novel model and prove new conditions on the structure of the network and model parameters that distinguish important dynamic regimes such as endemic, epidemic and infection-free. We demonstrate how this model can be used for disease prediction and how control strategies can be developed for disease mitigation.

Keywords: Neurodegenerative Disease, Brain Networks, Long-range Disease Agent Dispersal, Epidemic Modeling

1. INTRODUCTION

Understanding and predicting disease evolution in Alzheimer's (AD) disease is one of the most interesting research topics in our epoch. While many imaging techniques support AD diagnosis, there are still no reliable prediction models of disease progression. Two underlying hypotheses, the amyloid and tau hypotheses, are currently employed when it comes to describe the mechanism of AD. Brain imaging connectomics gives an impressive picture of the structural and functional changes related to AD. Describing dynamically the disease prediction relies mainly on two paradigms: (1) the heat-diffusion model and (2) the information-centric network paradigm in connection with an epidemic spreading model. Both paradigms comprise the transmission of disease agents (misfolded β -amyloid and τ -protein) over the connectome. Advanced control theory applied on brain networks have been shown to offer an excellent tool for analyzing the dynamics of disease by describing every node or brain region as an acting agent connected to the others. Pinning control mechanisms has been employed to determine the leader or driver nodes that are relevant for disease evolution.^{3,11,12} In previous work, the diffusion model was a heat-diffusion model.^{8,9} A detailed partial differential disease model of stochastic nature was presented in.^{2,7,10}

In this paper, we propose new model for the dynamical analysis and disease prediction based on epidemic models that accounts for long-range dispersal of disease agents propagation in brain networks. We pair two important concepts: the general SIRI (Susceptible-Infected-Recovered-Infected) epidemic model on a network of heterogeneous agents⁶ with the long-range dispersal of disease agents implemented based on transformations, such as the Mellin and Laplace transforms, which yield a generalization of the adjacency matrix of the geometric graph. We compare these results with brain regions in the structural networks that can act as drivers and move the system (brain) into specific states of action. These influence the cognitive functions. Our results will prove that the experimental neurological findings are confirmed by showing the correct diffusion sources for AD.^{13,14}

Corresponding Author: Anke Meyer-Baese

Pattern Recognition and Tracking XXXII, edited by Mohammad S. Alam,
Proceedings of SPIE Vol. 11735, 117350N · © 2021 SPIE
CCC code: 0277-786X/21/\$21 · doi: 10.1117/12.2588294

Proc. of SPIE Vol. 11735 117350N-1

2. MODELS OF PATHOGEN TRANSMISSION DYNAMICS ON HETEROGENEOUS SPATIALLY EMBEDDED NETWORKS

In control theory, a square matrix \mathcal{M} is of Hurwitz-type or stable if none of the eigenvalues have a positive or zero real part. A real square matrix \mathcal{M} is Metzler if $m_{jk} \geq 0$ for $j \neq k$. The spectrum of matrix \mathcal{M} is given as $\lambda(\mathcal{M}) = \{\lambda_1, \lambda_2, \dots, \lambda_N\}$, its spectral radius as $\rho(\mathcal{M}) = \max\{|\lambda_j| \mid \lambda_j \in \lambda(\mathcal{M})\}$ and the leading eigenvalue is $\lambda_{max}(\mathcal{M}) = \operatorname{argmax}_{\lambda_j \in \lambda(\mathcal{M})} |\lambda_j|$.

Properties of Metzler Matrices. Let K be a Metzler matrix. Then,

- $\lambda_{max}(K) \in \mathbb{R}$. If K is irreducible, then $\lambda_{max}(K)$ has multiplicity of one.
- K is Hurwitz.
- If K is a Metzler matrix and $K = T + U$ representing a regular splitting then:
 - (a) $\lambda_{max}(K) < 0$ if and only if $\rho(-TU^{-1}) < 1$.
 - (b) $\lambda_{max}(K) = 0$ if and only if $\rho(-TU^{-1}) = 1$.
 - (c) $\lambda_{max}(K) > 0$ if and only if $\rho(-TU^{-1}) > 1$.

To define the network model for the epidemiological SIR model describing a contagious process with reinfection, we consider a graph $\mathcal{G} = \{\mathcal{V}, \mathcal{E}\}$ with N nodes and adjacency matrix S . We use an individual-based mean-field approach (IBMF) as proposed in⁶ that assumes that the state of each node is statistically independent from its neighbors and describes the state of each agent j at time $t \geq 0$ as a probability $p_j^S(t), p_j^I(t), p_j^R(t)$ being in state S (susceptible), I (infected) or R (recovered). The probabilities are related as $p_j^S + p_j^I + p_j^R = 1$. By using this relationship, the number of state equations can be reduced from $3N$ to $2N$ and be written in matrix form with $p^\Omega = [p_1^\Omega, \dots, p_N^\Omega]^T$ and $P^\Omega = \operatorname{diag}(p^\Omega)$ for $\Omega \in \{S, I\}$:

$$\begin{aligned} \dot{p}^S &= -P^S B p^I \\ \dot{p}^I &= (B^*(p^S) - D)p^I - P^I \widehat{B} p^I \end{aligned} \quad (1)$$

where $B^*(p^S) = (\mathbf{1} - P^S)\widehat{B} + P^S B$

and

$$\begin{aligned} B &= \{\beta_{jk}\} \succeq \bar{\mathbf{0}} && \text{(infection matrix)} \\ \widehat{B} &= \{\beta_{jk}\} \succ \bar{\mathbf{0}} && \text{(reinfection matrix)} \\ D &= \operatorname{diag}\{\delta_1, \dots, \delta_N\} \succ \bar{\mathbf{0}} && \text{(recovery matrix)} \end{aligned} \quad (2)$$

As shown in,¹ we define the d -path adjacency matrix which describes the spread of infective particles from a given position beyond the immediate neighbors. d_{max} defines the graph diameter being the maximum shortest path distance in the disease graph.

We adopt the definition verbatim from:¹

Definition 1.¹ Let $d \leq d_{max}$. The p -th adjacency matrix, denoted by A_d , of a connected graph of N nodes is the square, symmetric $N \times N$ matrix whose entries are:

$$A_d(i, j) = \begin{cases} 1, & \text{if } d_{ij} = d \\ 0, & \text{otherwise} \end{cases}.$$

where d_{ij} is the shortest path distance between the nodes i and j .

The transformed d -path adjacency matrices for the Mellin and Laplace transforms are adopted from¹ as:

$$\tilde{A}^\tau = \begin{cases} \sum_{d=1}^{d_{max}} d^{-s} A_d, & \text{for } \tau = \text{Mell}, s > 0, \\ A + \sum_{d=2}^{d_{max}} \exp(-\lambda d) A_d, & \text{for } \tau = \text{Lapl}, \lambda > 0 \end{cases}$$

where τ the transformation's type as being either Mellin or Laplace.

The equations of the SIRI model under the individual mean-field approximation and considering that

The dynamics including the d-path adjacency matrices for the SIRI model where $p^\Omega = [p_1^\Omega, \dots, p_N^\Omega]$ and $P^\Omega = \text{diag}(p^\Omega)$ for $\Omega \in \{S, I\}$:

$$\begin{aligned} \dot{p}^S &= -P^S B \tilde{A}^\tau p^I \\ \dot{p}^I &= (B^* \tilde{A}^\tau(p^S) - D)p^I - P^I \hat{B} \tilde{A}^\tau p^I \end{aligned} \quad (3)$$

where $B^* \tilde{A}^\tau(p^S) = (\mathbf{1} - P^S) \tilde{A}^\tau \hat{B} + P^S B \tilde{A}^\tau$.

Two important models that pertain to neurodegenerative diseases can be derived from the SIRI network model:

- SI model: Assuming the matrix $D = 0$, the SIRI model becomes an SI model, meaning there is only infection or disease spread and no recovery.
- SIR model: Assuming $\hat{B} = 0$, the SIRI model becomes an SIR model, meaning there is also recovery.

The resulting equations for the SI and SIR models are:

$$\begin{aligned} \dot{p}^S &= -P^S B \tilde{A}^\tau p^I && \text{SIR model} \\ \dot{p}^I &= (P^S B \tilde{A}^\tau(p^S) - D)p^I \end{aligned} \quad (4)$$

and

$$\dot{p}^S = -P^S B \tilde{A}^\tau (1 - p^S) \quad \text{SI model} \quad (5)$$

3. EQUILIBRIA AND REPRODUCTION NUMBERS

The equilibria and reproduction numbers represent very important parameters describing the dynamical behavior of neurodegenerative models. The equilibrium values for p^S and p^I are defined as p^{S*} and p^{I*} , respectively.

Proposition 1.⁶ The only equilibria of the SIRI model (3) are the infection-free equilibria (IFE) and one or more isolated endemic equilibria (EE).

The IFE set is defined as

$$\mathcal{M} = \{(p^{S*}, \mathbf{0}) \in \Delta_N \mid \mathbf{0} \preceq p^{S*} \preceq \mathbf{1}\} \quad (6)$$

and corresponds to all equilibria for which $p^{I*} = \mathbf{0}$, i.e. $p^{S*} + p^{R*} = \mathbf{1}$.

EE represents the equilibria where $p^{I*} \succ \mathbf{0}$ satisfies

$$p_j^{I*} = \frac{\sum_{k=1}^N \hat{\beta}_{jk} \tilde{A}_{ij}^\tau p_k^{I*}}{\delta_j + \sum_{k=1}^N \hat{\beta}_{jk} \tilde{A}_{ij}^\tau p_k^{I*}} \quad (7)$$

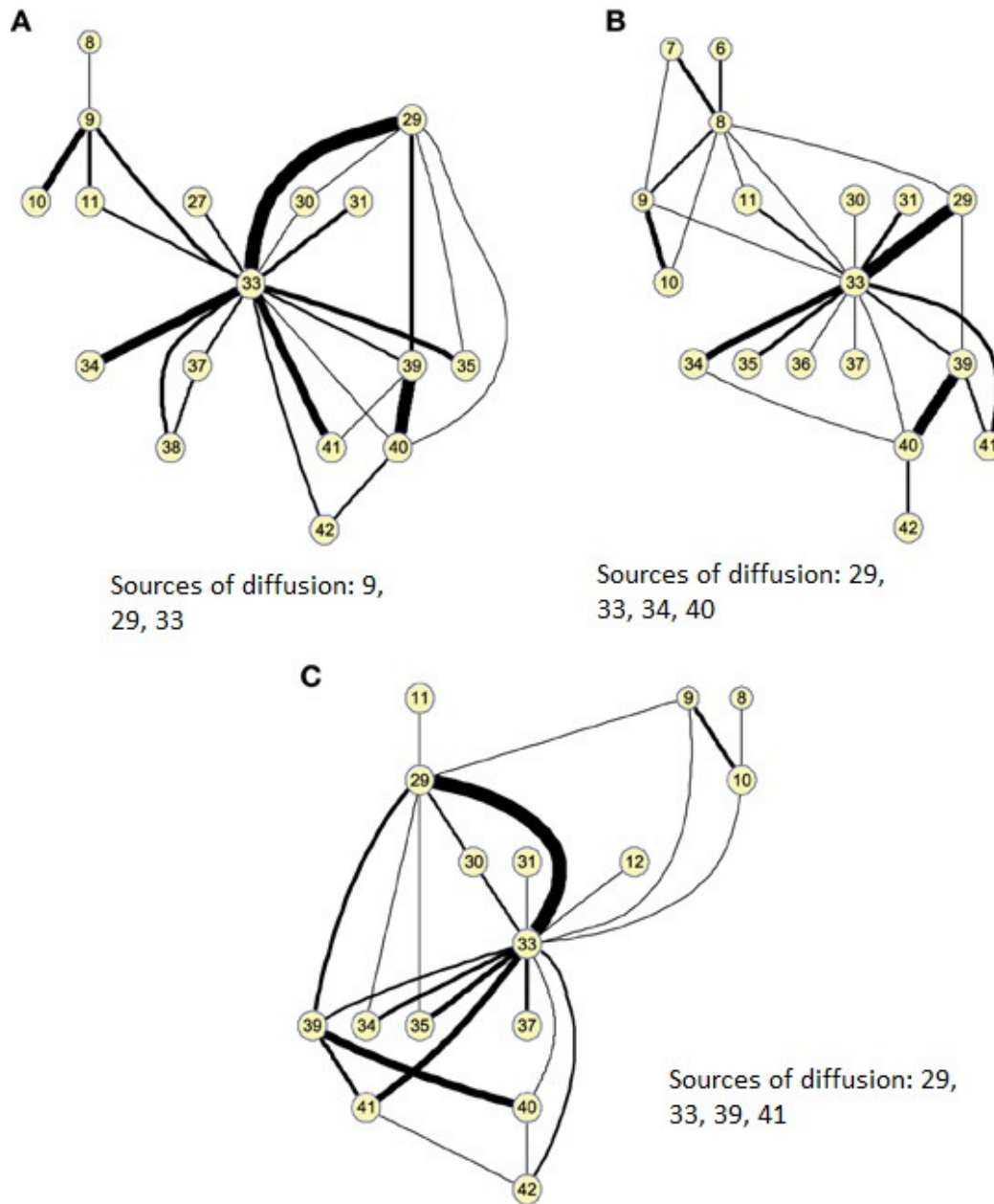


Figure 1: Nodes representing diffusion sources for a stochastic SI model.⁷

For \hat{B} irreducible, we have for every EE, $p^{S^*} = \mathbf{0}$ and $p^{I^*} \gg \mathbf{0}$.

Looking at the SI model, the only equilibrium is a unique EE where $p^{I^*} = \mathbf{1}$ and $p^{S^*} = \mathbf{0}$. And as for the SIR model, the only equilibria represent the IFE set \mathcal{M} .

The IFE stability for SIR on the set \mathcal{M} is determined based on the following Lemma.⁶

Lemma 1.⁶ (Local stability of points for the SIR model in the IFE set \mathcal{M}).

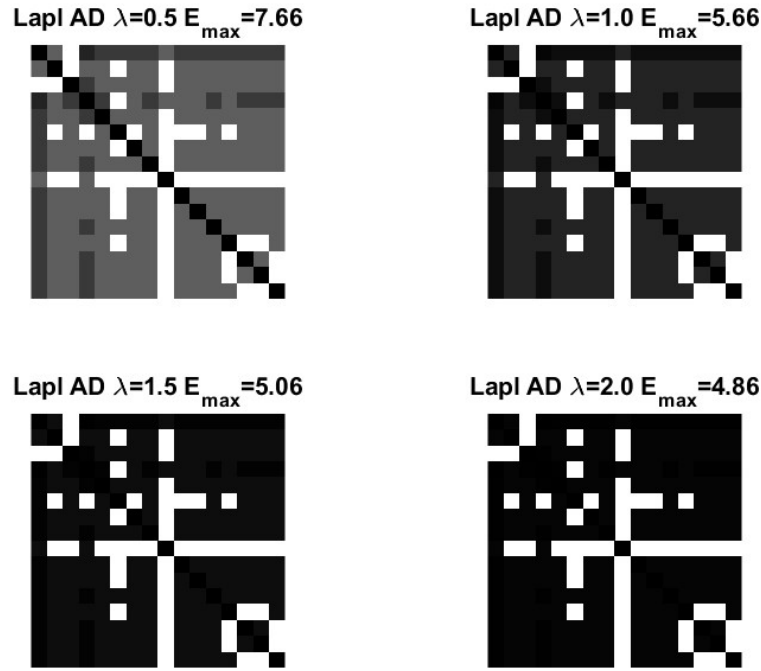


Figure 2: Laplace-transformed d -path adjacency matrix \tilde{A}^τ for $\lambda = 0.5, 1, 1.5, 2$.

Let $x = (p^{S^*}, \mathbf{0}) \in \mathcal{M}$. Let $J_{\mathcal{M}}(x)$ be the Jacobian of 4 at x and $\lambda_{Tmax}(J_{\mathcal{M}}(x))$ the leading transverse eigenvalue of $J_{\mathcal{M}}(x)$. Then $\lambda_{Tmax}(J_{\mathcal{M}}(x)) \in \mathbb{R}$ and the following hold.

- Suppose $\lambda_{Tmax}(J_{\mathcal{M}}(x)) < 0$, then x is locally stable.
- Suppose $\lambda_{Tmax}(J_{\mathcal{M}}(x)) > 0$, then x is unstable.

Proof. For an arbitrary point $x = (p^{S^*}, \mathbf{0}) \in \mathcal{M}$, we get for the SIR Jacobian $J_{\mathcal{M}}(x)$

$$J_{\mathcal{M}}(x) = \begin{bmatrix} \mathbf{0} & -P^{S^*} B \tilde{A}^\tau \\ \mathbf{0} & J_T(p^{S^*}) \end{bmatrix} \quad (8)$$

Since $J_T(p^{S^*}) = B^* \tilde{A}^\tau(p^{S^*}) - D = P^{S^*} B \tilde{A}^\tau - D$. The N transverse eigenvalues of $J_{\mathcal{M}}(x)$ are the eigenvalues of $J_T(p^{S^*})$ and thus $\lambda_{Tmax}(J_{\mathcal{M}}(x)) = \lambda_{max}(J_T(p^{S^*}))$. As shown in,⁶ if $\lambda_{max}(J_T(p^{S^*})) < 0$, then every transverse eigenvalue of $J_{\mathcal{M}}(x)$ has a negative real part. The contrary happens if $\lambda_{max}(J_T(p^{S^*})) > 0$, then there exists at least one transverse eigenvalue of $J_{\mathcal{M}}(x)$ with positive real part.

We use the definitions from⁶ and describe the basic R_0 and extreme basic reproduction numbers R_{max} and R_{min} to analyze the SIR dynamical behavior. Their computation is based on the spectral radius formulas from the below Proposition.

Proposition 2.1 (Spectral Radius Formulas for Reproduction Numbers). The reproduction numbers for a SIR model are given as following:

- $R_0 = \rho(B \tilde{A}^\tau D^{-1})$
- $R_{max} = \max_{\mathbf{0} \leq p \leq \mathbf{1}} \rho(P B \tilde{A}^\tau D^{-1})$
- $R_{min} = \min_{\mathbf{0} \leq p \leq \mathbf{1}} \rho(P B \tilde{A}^\tau D^{-1})$

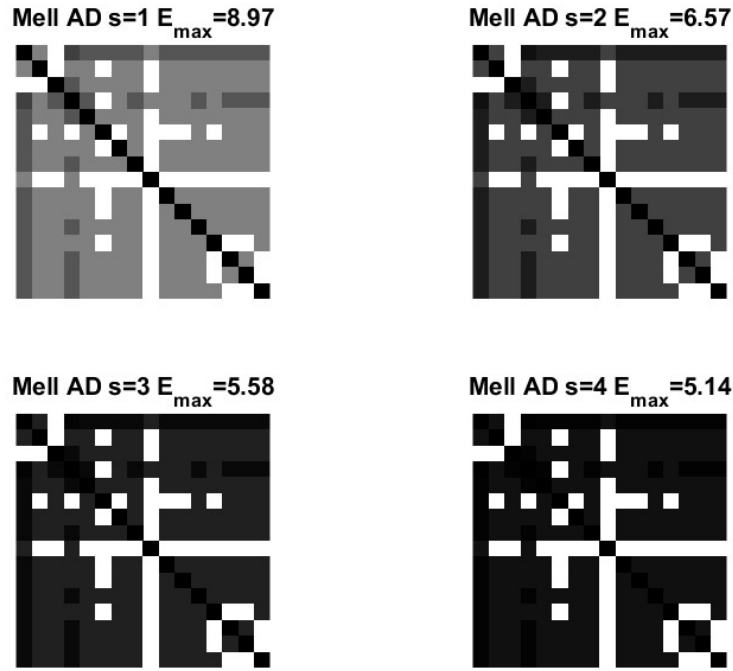


Figure 3: Mellin-transformed d -path adjacency matrix \tilde{A}^τ for $s = 1, 2, 3, 4$.

where $P = \text{diag}(p)$.

As a consequence of the above definitions and the derivations from,⁶ we obtain:

- SI model: $R_{\min} > 1$ and all solutions of (3) converge to the endemic regime.
- SIR model: $R_{\max} = R_0$ and $R_{\min} = 0$. The only solutions converge to the infection-free and epidemic regimes.

The epidemic threshold $\zeta = \frac{\beta}{\delta}$ is a marker for determining when an infection dies out: if $\zeta < 1$, the infection dies out and when $\zeta > 1$ the infection becomes an epidemic. In⁴ was shown that $\zeta = \frac{1}{\lambda_1(G)}$ with λ_1 being the largest eigenvalue for the adjacency matrix. For the transformed d -path adjacency matrix \tilde{A}^τ , it was shown in¹ that the same relationship holds when the regular adjacency matrix is replaced by the transformed matrix.

In the dementia environment, we have the following control mechanisms for the recovery steady state: (1) modification of the brain region recovery rate, (2) modification of the region's disease agent transmission rate and (3) modification of the affected brain connectome topology.

4. RESULTS

We apply the theoretical results on structural (MRI) connectivity graphs for control (CN), mild cognitive impairment (MCI) and Alzheimer's disease (AD) subjects. For the structural data, the connections in the graph show the inter-regional covariation of gray matter volumes in different areas. We considered only 42 out of the 116 from the AAL in the frontal, parietal, occipital and temporal lobes as shown in.⁵ The nodes in the graphs represent the regions while the links show if a connection is existing between these regions or not. Figure 1 (a)-(c) shows the sources found on the structural data for (A) controls, (B) MCI and (3) AD based on an SI mode.

We apply the Mellin- and Laplace-transformations on the adjacency matrices and the resulting graphs are shown in Figures 2 and 3 for different parameter's values. The epidemic thresholds change in function of the parameters of each transform. Table 1 shows the epidemic threshold for varying parameters for the two transforms. For both transforms the epidemic threshold increases when the specific Mellin and Laplace parameters increase.

Table 1: Epidemic threshold for the two transformed d -path adjacency matrix \tilde{A}^τ Mellin and Laplace for varying parameters for AD.

Mellin transform	Laplace transform
s=1: 0.11	$\lambda = 0.5$: 0.13
s=2: 0.15	$\lambda = 1$: 0.17
s=3: 0.17	$\lambda = 1.5$: 0.17
s=4: 0.19	$\lambda = 2$: 0.19

Figures 2 and 3 representing the transformed adjacency matrices show that the spread of the infective particle beyond the nearest neighbors from its current position is stronger for the Laplace transformation than for the Mellin transformation.

5. CONCLUSIONS

In this paper, we have developed a novel disease transmission model for dementia on heterogenous spatially embedded networks that takes into account the long-range transmission of disease agents. The model represents a special case of a general SIRI model by using a transformed adjacency matrices. The spatial characteristics is implemented by applying transformations, such as the Mellin and Laplace transforms on the adjacency matrix. We analyze two special cases, the SI and SIR model, and derive the epidemic parameters. In the case of the SI model, we have shown that the spread of the infective particle beyond the nearest neighbors from its current position favors the Laplace transformation than the Mellin transformation. We hypothesize that we have for this transformed model a much faster propagation of the disease than in normal diffusion models for dementia.

6. CONFLICT OF INTEREST STATEMENT

The authors declare that the research was conducted in the absence of any commercial or financial relationships that could be construed as a potential conflict of interest.

REFERENCES

- [1] Juddy H Arias, Jesus Gómez-Gardeñes, Sandro Meloni, and Ernesto Estrada. Epidemics on plants: Modeling long-range dispersal on spatially embedded networks. *Journal of theoretical biology*, 453:1–13, 2018.
- [2] J. Hu, Q. Zhang, A. Meyer-Baese, and M. Ye. Stationary distribution of a stochastic alzheimer’s disease model. *Mathematical Methods in the Applied Sciences*, 43:9706–9718, 1 2020.
- [3] A. Meyer-Baese, I. A. Illan, and A. Stadlbauer. Dynamical graph theory networks methods for the analysis of sparse functional connectivity networks and for determining pinning observability in brain networks. *Frontiers in Computational Neuroscience*, page accepted for publication, 1 2016.
- [4] P. V. Mieghem, J. Omic, and R. Kooij. Virus spread in networks. *IEEE/ACM Transactions on Networking*, 17:1–14, 1 2009.
- [5] A. Ortiz, J. Munilla, I. Alvarez-Illan, M. Gorriz, and J. Ramirez. Exploratory graphical models of functional and structural connectivity patterns for alzheimer’s disease diagnosis. *Frontiers in Computational Neuroscience*, <http://dx.doi.org/10.3389/fncom.2015.00132>, 1 2015.
- [6] Renato Pagliara and Naomi Ehrlich Leonard. Adaptive susceptibility and heterogeneity in contagion models on networks. *IEEE Transactions on Automatic Control*, 2020.
- [7] L. Van Poppering, A. Tahmassebi, and A. Meyer-Baese. Identifying the diffusion source of dementia spreading in structural brain networks. *Proc. SPIE Medical Imaging*, page In Press, 1 2021.
- [8] A. Raj and P. Fon. Models of network spread and network degeneration in brain disorders. *Biol Psychiatry Cogn Neurosci Neuroimaging*, 3:788–797, 1 2018.
- [9] A. Raj, E. LoCastro, N. Relkin, and M. Weiner. Network diffusion model of progression predicts longitudinal patterns of atrophy and metabolism in alzheimer’s disease. *Cell Reports*, 10:359–369, 1 2015.
- [10] A. Tahmassebi, U. Meyer-Baese, and A. Meyer-Baese. Modeling disease spreading process induced by disease agent mobility in dementia networks. *Proc. SPIE 11400*, DOI:10.1117/12.2557814, 1 2020.
- [11] A. Tahmassebi, A. Moradi Amani, K. Pinker-Domenig, and A. Meyer-Baese. Determining disease evolution driver nodes in dementia networks. *Proc. SPIE 10578, Medical Imaging*, DOI:10.1117/12.2293865, 1 2018.
- [12] A. Tahmassebi, B. Mohebbali, L. Meyer-Baese, P. Solimine, K. Pinker, and A. Meyer-Baese. Determining driver nodes in dynamic signed biological networks. *Proc. SPIE 11020*, 11020A, 1 2019.
- [13] A. Tahmassebi, K. Pinker-Domenig, G. Wengert, M. Lobbes, A. Stadlbauer, F. Romero, D. Morales, E. Castillo, A. Garcia, G. Botella, et al. Dynamical graph theory networks techniques for the analysis of sparse connectivity networks in dementia. In *Smart Biomedical and Physiological Sensor Technology XIV*, volume 10216, page 1021609. International Society for Optics and Photonics, 2017.
- [14] A. Tahmassebi, K. Pinker-Domenig, G. Wengert, M. Lobbes, A. Stadlbauer, N. C Wildburger, F. Romero, D. Morales, E. Castillo, A. Garcia, et al. The driving regulators of the connectivity protein network of brain malignancies. In *Smart Biomedical and Physiological Sensor Technology XIV*, volume 10216, page 1021605. International Society for Optics and Photonics, 2017.